Available online at www.sciencedirect.com
ScienceDirect
Ceramics International 36 (2010) 2235–2239
CERAMICS INTERNATIONAL
www.elsevier.com/locate/ceramint

Short communication

Oxidation behavior of Al_2O_3 reinforced $MoSi_2$ composite coatings fabricated by vacuum plasma spraying

Xiaoai Fei [a,b], Yaran Niu [a,b], Heng Ji [a,b], Liping Huang [a,b], Xuebin Zheng [a,b,*]

[a] Key Laboratory of Inorganic Coating Materials, Chinese Academy of Sciences, Shanghai 200050, China
[b] Shanghai Institute of Ceramics, Chinese Academy of Sciences, Shanghai 200050, China

Received 14 December 2009; received in revised form 6 March 2010; accepted 16 April 2010
Available online 21 May 2010

Abstract

$MoSi_2$, $MoSi_2$–10 vol.% Al_2O_3, $MoSi_2$–30 vol.% Al_2O_3 (denoted as MA0, MA1, MA3, respectively) coatings were fabricated by vacuum plasma spraying (VPS), and their oxidation behavior was examined at low temperature (500 °C) and high temperature (1500 °C). The test at 500 °C showed that the addition of Al_2O_3 effectively restrained the pest oxidation of $MoSi_2$. The MA1 coating had satisfactory fluid surface and presented good oxidation resistance at 1500 °C. However, the MA3 coating showed worse oxidation resistant behavior compared with the MA0 coating because of mullite formation.
Published by Elsevier Ltd and Techna Group S.r.l.

Keywords: D. Al_2O_3; $MoSi_2$; Coatings; Vacuum plasma spraying; Oxidation behavior

1. Introduction

$MoSi_2$ has been extensively researched during the last 30 years for its rather low density, high electrical conductivity and very good oxidation resistance at high temperature, even in aggressive environments [1]. It has been widely used as heating elements operating at high temperatures, and in gas turbine engines, missile nozzles, diesel engine grow plugs and so on [2]. One of its important applications was as oxidation resistant aerospace coating. Via the formation of a thin protective SiO_2 layer, $MoSi_2$ can protect materials from further oxidation [3].

Many coating techniques have been suggested to fabricate $MoSi_2$, such as pack siliconizing, plasma spraying and chemical vapor deposition [4–6]. Among the various coating methods, plasma spraying is the most flexible thermal spray process with respect to the sprayed materials. The high temperature of plasma spray processes permits the deposition of coatings for applications in areas of liquid and high temperature corrosion and oxidation protection and also for thermal, electrical and biomedical purposes [7].

Unfortunately some engineering drawbacks for $MoSi_2$ coatings, such as ''pest'' oxidation at low temperature (400–600 °C), relatively high porosity and amorphous SiO_2 crystallization, limited their applications [8]. Catastrophic nature of the pest oxidation was proposed to occur through transport of oxygen into the interior of $MoSi_2$ along pre-existing cracks, grain boundaries, and/or pores, which was accomplished with volume expansion of about 250% [9–11]. Therefore, coating systems to bestow adequate oxidation resistance are required. Among the various methods, the fabrication of composite coatings was potentially useful [12]. The introduction of Al_2O_3 into the $MoSi_2$ matrix as second phase is focused in our research. The network microstructure of oxides was supposed to block the paths of oxygen diffusion that caused pest oxidation at the low-temperature (around 500 °C) [13]. Besides, Al_2O_3 has proved to be effective for adjusting viscosity and improving the crystallization temperature of SiO_2 [14]. Furthermore, the excellent match of the coefficients of thermal expansion of the two oxides and related absence of residual thermal stresses during sintering and cooling ensured the $MoSi_2$–Al_2O_3 system to be stable up to 1600 °C [15]. However, there are limited data on the effect of Al_2O_3 addition on the oxidation resistance of $MoSi_2$ coatings. The purpose of this work was to investigate the oxidation behavior of $MoSi_2$ coating with different amounts of Al_2O_3 additions. $MoSi_2$

* Corresponding author at: Key Laboratory of Inorganic Coating Materials, Chinese Academy of Sciences, Shanghai 200050, China. Tel.: +86 52411050.
E-mail addresses: xiaoaif@yahoo.cn (X. Fei), xbzheng@mail.sic.ac.cn (X. Zheng).

0272-8842/$36.00. Published by Elsevier Ltd and Techna Group S.r.l.
doi:10.1016/j.ceramint.2010.05.001

coating without Al_2O_3 reinforcement was prepared as well for comparison.

2. Experimental procedures

Commercial $MoSi_2$ (Zhengzhou Chida Tungsten & Molybdenum Products Co., Ltd., China) and Al_2O_3 (Anyan Tianchuang Hot spray Products Co., Ltd., China) powders were chosen in the range of 10–40 μm. $MoSi_2$ with 10 vol.% and 30 vol.% Al_2O_3 powders were mixed in a ball mill for 12 h, then dried at 110 °C for 2 h. The deposition of coatings was carried out with a vacuum plasma spraying equipment (F4-VB, Sulzer Metco AG, Switzerland). Optimized deposition parameters of coatings are summarized in Table 1. Free-standing coatings of thickness about 0.5–1.0 mm were fabricated for the oxidation studies.

The crystalline phases of the powders and coatings were analyzed by X-ray diffraction (XRD, RAX-10, Rigaku, Japan). The surface and cross-section morphologies of the as-sprayed and heat-treated coatings were investigated by field emission scanning electron microscopy (FE-SEM, JSM-6700F, JEOL, Japan).

3. Results and discussion

3.1. Characterization of powders and coatings before oxidation

Fig. 1 shows the surface (a, c and e) and cross-section (b, d and f) morphologies of the as-sprayed coatings. The surfaces of the MA0 (0% Al_2O_3) and MA3 (30% Al_2O_3 addition) coatings constituted of insufficiently flattened protuberances and unmelted particles. However, the MA1 (10% Al_2O_3 addition) coating presented a comparatively different surface. Lamellar structure, which is a common character of plasma sprayed coatings was also observed from the cross-section morphologies. It was worth noticing that the MA1 coating had a finer structure compared with the MA0 and MA3 coatings.

Table 1
Spraying parameters of $MoSi_2$–Al_2O_3 coatings.

Parameters	Values
Power (kw)	35
Gas Ar (slpm)	42
Gas H_2 (slpm)	10
Spraying distance (mm)	300
Carrier gas Ar (slpm)	4
Pressure (mbar)	100

The XRD patterns of the powders and of the as-sprayed coatings are compared in Fig. 2. Tetragonal $MoSi_2$ and small amount of Mo_5Si_3 could be found in all the three kinds of powders. A small reflection of Al_2O_3 was detected in the MA1 and MA3 powders. The XRD patterns of the MA0, MA1 and MA3 coatings showed: (i) $MoSi_2$ with a hexagonal lattice as the main phase, (ii) more Mo_5Si_3 as compared with the starting powders, and (iii) the reflections of Al_2O_3 appeared in the MA1 and MA3 coatings too. Due to ultrahigh temperature of the plasma plume and high cooling rate of the molten particles in spraying process, the high temperature hexagonal $MoSi_2$ was found to exist as the main phase in the coatings. The chemical reaction between $MoSi_2$ and residual O_2 in the vacuum chamber may contribute to the increase of the content of Mo_5Si_3 (Eq. (1)) [16].

$$5MoSi_{2(s)} + 7O_{2(g)} \rightarrow Mo_5Si_{3(s)} + 7SiO_{2(s)} \quad (1)$$

3.2. Oxidation behavior of coatings at low temperature (500 °C)

The oxidation behavior at 500 °C was tested on the three kinds of coatings. Fig. 3 presents the surface morphologies of the oxidized coatings. The MA0 coating (Fig. 3a) disintegrated into a green powder with small rests of the original coating, oui volume increasing dramatically after 16 h oxidation. A higher magnification of Fig. 3a (Fig. 3d) shows MoO_3-whiskers or

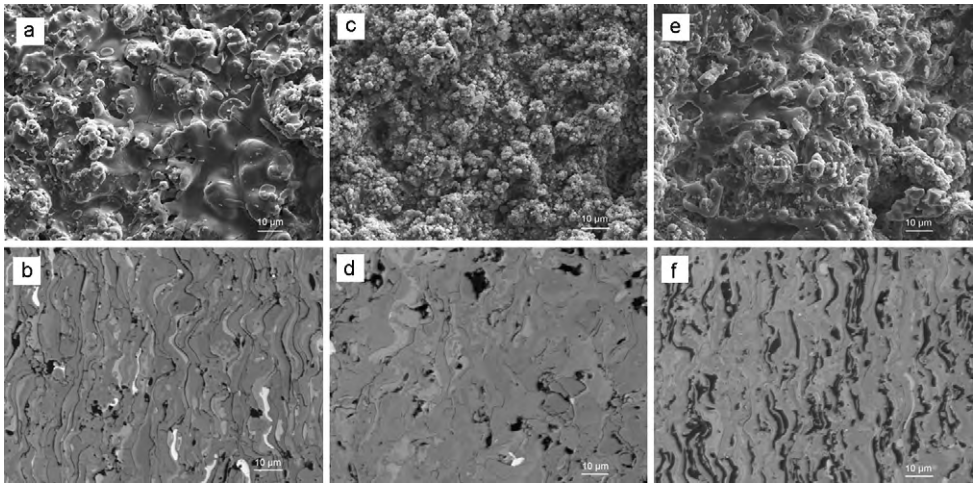

Fig. 1. Surface (a, c and e) and cross-section (b, d and f) morphologies of the as-sprayed coatings: (a and b) MA0 (0% Al_2O_3), (c and d) MA1 (10% Al_2O_3), (e and f) MA3 (30% Al_2O_3).

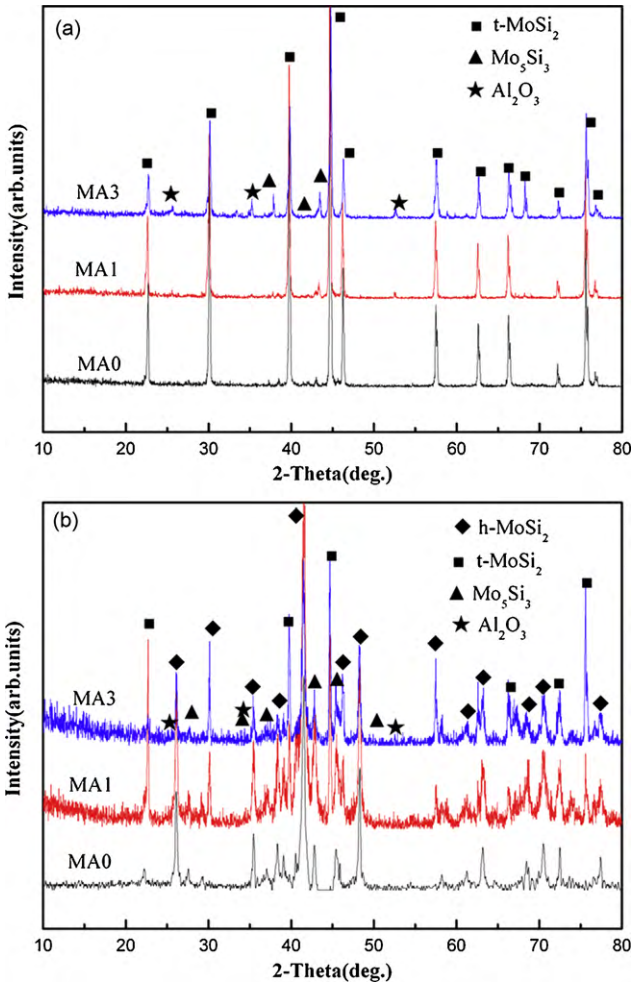

Fig. 2. XRD patterns of (a) the powders and (b) the corresponding coatings.

platelets and amorphous SiO_2-clusters, which are typical products of pest oxidation [10]. This phenomenon of pest oxidation well known for monolithic $MoSi_2$ didn't happen in the MA1 and MA3 coatings until 48 h, which meant that the addition of Al_2O_3 in the $MoSi_2$ coating could effectively restrain its pest oxidation. Fig. 4 compares the XRD patterns of the three kinds of coatings after the oxidation test. MoO_3 was detected as the main phase in the MA0 coating, and a small amount of Mo_5Si_3 and residual tetragonal $MoSi_2$ were also found. However, $MoSi_2$ and MoO_3 were found as main phases in the MA1 and MA3 coatings whose intensity in MA0 coating was much lower than the MA1 and MA3 coatings. However, no diffraction peak of Al_2O_3 was detected. No reflections of Al_2O_3 appeared in Al_2O_3-SiO_2 thin films deposited by E-beam evaporation too [14]. But the reason for the absence of Al_2O_3 peaks need to be further investigated.

3.3. Oxidation behavior of coatings at high temperature (1500 °C)

The oxidation behavior of the coatings at 1500 °C was also studied. Mass change curve of MA0, MA1 and MA3 coatings at 1500 °C is shown in Fig. 5. After oxidation for 30 h, the mass gains of the MA0, MA1 and MA3 coatings were 1.45, 1.41 and 1.70 mg/cm^2, respectively. The oxidation rate of the MA1 coating was lower than the MA0 and MA3 coatings.

The surface (a, c and e) and cross-section (b, d and f) morphologies of the coatings which were oxidized at 1500 °C for 7 h are illustrated in Fig. 6. The MA1 coatings had a much smoother and denser surface compared to the MA0 and MA3 coatings. However, the MA3 coating presented a porous surface. The cross-section micrographs of the three coatings show that a thicker oxide layer was formed on the surface of the

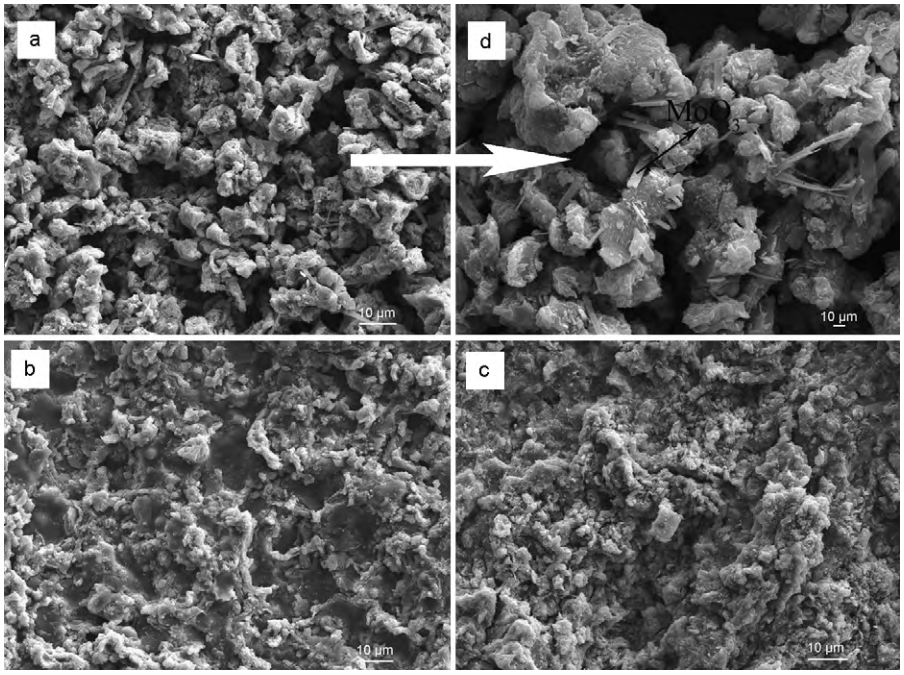

Fig. 3. Surface morphologies of coatings heated at 500 °C for 16 h: (a) MA0, (b) MA1, (c) MA3 and (d) higher magnification of (a).

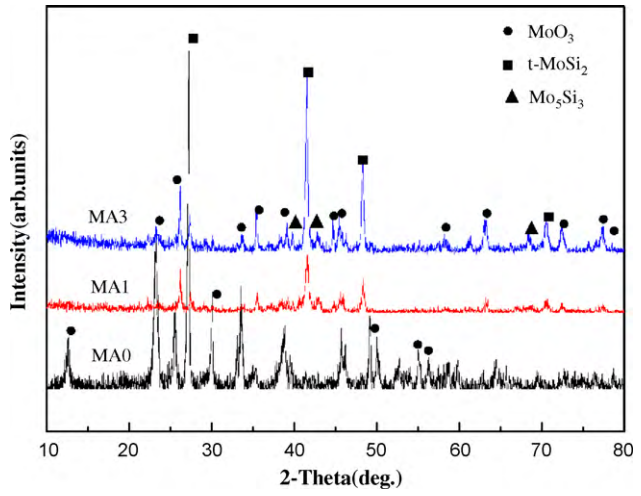

Fig. 4. XRD Patterns of MA0, MA1 and MA3 coatings heated at 500 °C for 16 h.

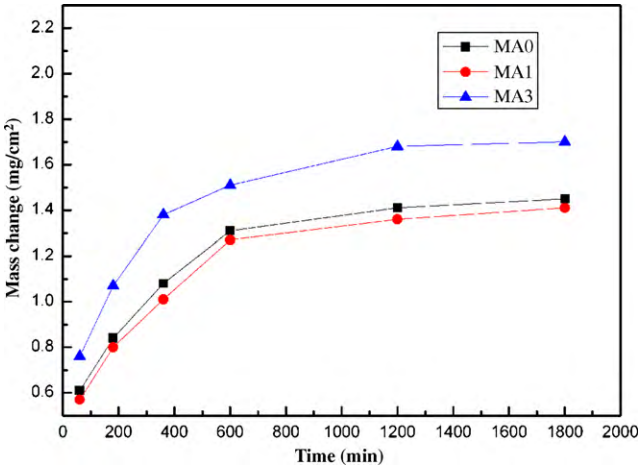

Fig. 5. Mass change curve of MA0, MA1 and MA3 coatings at 1500 °C.

MA3 coating compared with the MA0 and MA1 coatings, indicating that the MA3 coating had the worst oxidation resistance among the three coatings. Mo_5Si_3, tetragonal $MoSi_2$ and SiO_2 were detected by XRD in all the three coatings

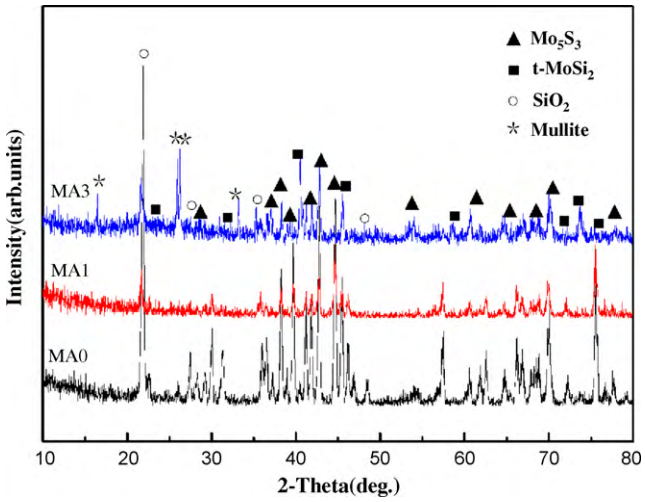

Fig. 7. XRD patterns of MA0, MA1 and MA3 coatings heated at 1500 °C for 7 h.

(Fig. 7). At the same time, mullite was found in the MA3 coating because of the reaction between Al_2O_3 and thermally grown SiO_2 [17].

It is suggested that minor amounts of Al_2O_3 may have important effects on the glass forming ability of the batch, its crystallization behavior and the tendency to phase separation during casting or reheating of the glass, which may alter the type and amount of the crystallized phases and consequently affect the properties of the product [18]. An investigation [19] of the effect of Al_2O_3 in the matrix of molybdenum and tungsten disilicides on modifying the structure and oxidation resistance of the coatings at high temperatures showed that SiO_2 film alloyed with Al_2O_3 formed over the modified coatings at the beginning of the oxidation. Higher thermal stability, higher crystallization temperature and better protective properties were got compared to the pure SiO_2 film formed on the surface of the unmodified silicide coatings. However, mullite was formed with increased amount of Al_2O_3 (30 vol.%), which resulted in a porous surface of the oxide layer. The integrality of SiO_2 protective film was destroyed and the oxidation resistant capacity of $MoSi_2$ was reduced.

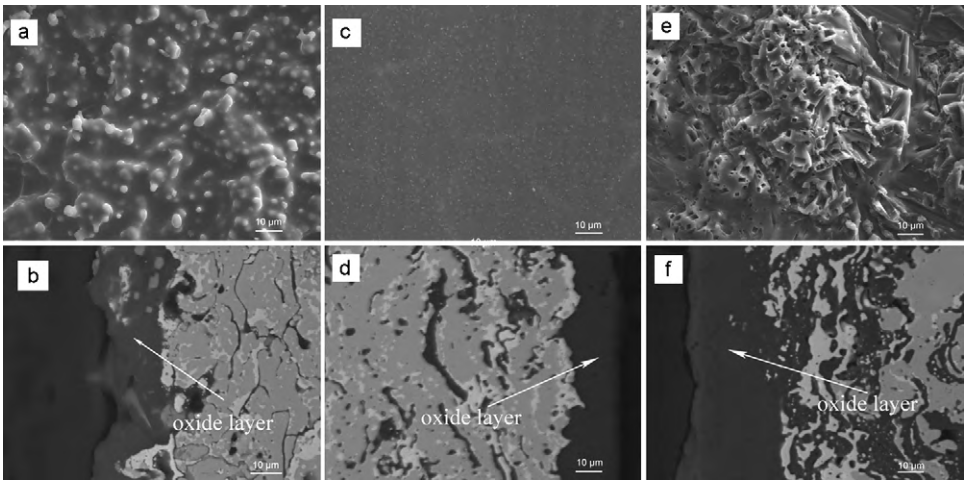

Fig. 6. Surface (a, c and e) and cross-section (b, d and f) morphologies of coatings heated at 1500 °C for 7 h: (a) MA0, (b) MA1 and (c) MA3.

4. Conclusions

$MoSi_2$–Al_2O_3 composite coatings were fabricated by vacuum plasma spraying. The addition of Al_2O_3 could effectively restrain the pest oxidation of $MoSi_2$ at low temperature (500 °C). The addition of 10 vol.% Al_2O_3 dispersed in thermally grown SiO_2 enhanced the fluidity of glass, which guaranteed a good oxidation resistance at 1500 °C. However, excess addition of Al_2O_3 (30 vol.%) into $MoSi_2$ severely affected its oxidation resistance at high temperature because of mullite formation.

References

[1] A.L. Dumont, J.P. Bonnet, T. Chartier, $MoSi_2/Al_2O_3$ FGM: elaboration by tape casting and SHS, J. Eur. Ceram. Soc. 21 (2001) 2353–2360.

[2] E.K. Nyutu, M.A. Kmetz, S.L. Suib, Formation of $MoSi_2$–SiO_2 coatings on molybdenum substrates by CVD/MOCVD, Surf. Coat. Technol. 200 (2006) 3980–3986.

[3] Z.D. Liu, S.X. Hou, D.Y. Liu, L.P. Zhao, B. Li, J.J. Liu, An experimental study on synthesizing submicron $MoSi_2$-based coatings using electrothermal explosion ultra-high speed spraying method, Surf. Coat. Technol. 202 (2008) 2917–2921.

[4] J.K. Yoon, K.H. Lee, G.H. Kim, J.K. Lee, J.M. Doh, K.J. Hong, Growth kinetics of $MoSi_2$ coating formed by a pack siliconizing process, J. Electrochem. Soc. 151B (2004) 309–318.

[5] R. Tiwari, H. Herman, S. Sampath, Vacuum plasma spraying of $MoSi_2$ and its composite, Mater. Sci. Eng. 155A (1992) 95–100.

[6] G.A. West, K.W. Beeson, Chemical vapor deposition of molybdenum silicide, J. Electrochem. Soc. 135 (7) (1988) 1752–1757.

[7] H. singh, S. Prakash, D. Puri, Some observations on the high temperature oxidation behavior of plasma sprayed Ni_3Al coatings, Mater. Sci. Eng. 444A (2007) 242–250.

[8] D.A. Berztiss, R.R. Cerchiara, E.A. Gulbransen, F.S. Pettit, G.H. Meier, Oxidation of $MoSi_2$ and comparison with other silicide materials, Mater. Sci. Eng. 155A (1992) 165–181.

[9] J.H. Westbrook, D.L. Wood, "PEST" degradation in beryllides, silicides, aluminides, and related compounds, J. Nucl. Mater. 12 (1964) 208–215.

[10] C.G. McKamey, P.F. Tortorelli, J.H. DeVan, C.A. Carmichael, Study of pest oxidation in polycrystalline $MoSi_2$, J. Mater. Res. 7 (10) (1992) 2747–2755.

[11] T.G. Chou, T.G. Nieh, Mechanism of $MoSi_2$ pest during low temperature oxidation, J. Mater. Res. 8 (1) (1993) 214–226.

[12] J.K. Yoon, G.H. Kim, J.H. Han, I.J. Shon, J.M. Doh, K.T. Hong, Low-temperature cyclic oxidation behavior of $MoSi_2/Si_3N_4$ nanocomposite coating formed on Mo substrate at 773 K, Surf. Coat. Technol. 200 (2005) 2537–2546.

[13] G. Wang, W. Jiang, G. Bai, L. Wu, Effect of addition of oxides on low-temperature oxidation of molybdenum disilicide, J. Am. Ceram. Soc. 86 (4) (2003) 731–734.

[14] H.H. Huang, Y.S. Liu, Y.M. Chen, M.C. Huang, M.C. Wang, Effect of oxygen pressure on the microstructure and properties of the Al_2O_3–SiO_2 thin films deposited by E-beam evaporation, Surf. Coat. Technol. 200 (2006) 3309–3313.

[15] S. Köbel, J. Plüschke, U. Vogt, T.J. Graule, $MoSi_2$–Al_2O_3 electroconductive ceramic composites, Ceram. Int. 30 (2004) 2105–2110.

[16] G. Reisel, B. Wielage, S. Steinhäuser, I. Morgenthal, R. Scholl, High temperature oxidation behavior of HVOF-sprayed unreinforced and reinforced molybdenum disilicide powders, Surf. Coat. Technol. 146 (2001) 19–26.

[17] G. Chen, H. Qi, W.H. Xing, N.P. Xu, Direct preparation of macroporous mullite supports for membranes by in situ reaction sintering, J. Membr. Sci. 318 (2008) 38–44.

[18] E. Demirkesen, E. Maytalman, Effect of Al_2O_3 additions on the crystallization behaviour and bending strength of a Li_2O–ZnO–SiO_2 glass–ceramic, Ceram. Int. 27 (2001) 99–104.

[19] V.I. Zmii, A.P. Patokin, V.L. Khrebtov, B.M. Shirokov, Molybdenum-based oxidation-resistant oxidation $MoSi_2$–Al_2O_3 and WSi_2–Al_2O_3 coatings, Powder Metall. Met. Ceram. 47 (2008) 11–12.